

Estimation of Rotor Loads Due to Wake Steering

Jonathan R. White¹, Brandon L. Ennis² and Thomas G. Herges³
Sandia National Laboratories⁴, Albuquerque, NM, 87112

To reduce the levelized cost of wind energy, wind plant controllers are being developed to improve overall performance by increasing energy capture. Previous work has shown that increased energy capture is possible by steering the wake around downwind turbines; however, the impact this steering action has on the loading of the turbines continues to need further investigation with operational data to determine overall benefit. In this work, rotor loading data from a wind turbine operating a wake steering wind plant controller at the DOE/Sandia National Laboratories Scaled Wind Farm Technology (SWiFT) Facility is evaluated. Rotor loading is estimated from fiber optic strain sensors acquired with a state-of-the-art Micron Optics Hyperion interrogator mounted within the rotor and synchronized to the open-source SWiFT controller. A variety of ground and operational calibrations were performed to produce accurate measurements of rotor blade root strains. Time- and rotational-domain signal processing methods were used to estimate bending moment at the root of the rotor blade. Results indicate a correlation of wake steering angle with: one-per-revolution thrust moment amplitude, two-per-revolution torque phase, and three-per-revolution torque amplitude and phase. Future work is needed to fully explain the correlations observed in this work and study additional multi-variable relationships that may also exist.

Nomenclature

<i>CTE</i>	= Coefficient of Thermal Expansion
<i>DOE</i>	= US Department of Energy
<i>FBG</i>	= Fiber Bragg Grating
<i>Sandia</i>	= Sandia National Laboratories
<i>SWiFT</i>	= Sandia Scaled Wind Farm Technology Facility

I. Introduction

At the end of 2016 the US wind capacity topped 82,183 megawatts (MW) and accounted for 4.7% of all electricity generated. In the state of Iowa, more than 30% of the state's energy consumption came from wind. Wind energy growth trends are expected to continue into the future. As wind becomes a dominant generation source, the performance and reliability of wind plants is increasingly important for electric grid stability. The Department of Energy (DOE) Wind Energy Technologies Office is leading the effort to develop breakthrough technologies, such as advanced rotors and wind plant controllers that will enable this growth of wind plant production onto the grid through the Atmosphere to Electrons program.

Some wind plants underperform their designed power production and one of the sources of underperformance is uncertainty in the effect of the velocity deficit behind wind turbines, known as the turbine wake. Currently, efforts are being made to improve the model predictions of wakes and to deploy wind plant controllers that control the wakes using a variety of methods. One method is wake steering, in which the turbine rotor is intentionally angled away from facing the wind to steer the wake around a downwind turbine. In a different method, induction control changes the rotor blade pitch and speed to alter the magnitude of the wake deficit. Lastly, tilt control angles the turbine rotor

¹ Principal Member of the Technical Staff, Wind Energy Department, PO Box 5800 MS1124.

² Senior Member of the Technical Staff, Wind Energy Department, PO Box 5800 MS1124.

³ Senior Member of the Technical Staff, Wind Energy Department, PO Box 5800 MS1124.

⁴ Sandia National Laboratories is a multimission laboratory managed and operated by National Technology and Engineering Solutions of Sandia, LLC., a wholly owned subsidiary of Honeywell International, Inc., for the U.S. Department of Energy's National Nuclear Security Administration under contract DE-NA-0003525.

towards the sky, thereby, steering the wake towards the ground and possibly encouraging recovery of wake deficits by entraining higher velocity winds above the turbine. For the work detailed within this document, a wake steering controller [1] [2] was demonstrated on an upwind/downwind pair of wind turbines at the DOE Sandia Scaled Wind Farm Technology Facility (SWiFT) [3]. The degree to which wake steering was implemented was quantified as the yaw offset angle. The yaw offset angle is defined as the angle between the rotor heading and wind inflow angle.

The SWiFT Facility is the premier and only purpose-built facility for testing wind plant technology innovations. A partnership between Sandia National Laboratories and the National Renewable Energy Laboratory developed a wake steering controller that was deployed on the public open-source wind turbines at SWiFT. The field testing campaign leveraged the extensive instrumentation network at SWiFT, as well as a unique scanning LIDAR from the Technical University of Denmark. The focus of this paper is to analyze rotor structural loading as measured by a state-of-the-art Micron Optics Hyperion Fiber Optic Interrogator and fiber optic strain gages. This paper also covers, methods used to improve the accuracy of the data as well as the methods for extracting features are described.

Several studies have been performed using fiber-optic sensing. Lading et al. [4] and Verbruggen et al. [5] proposed online condition monitoring in 2002 - 2003 and recognized the potential for fiber optic sensors. Schroeder et al. [6] installed an array of fiber Bragg gratings (FBG) on a 4.5 MW turbine in 2006 and demonstrated successful measurement of bending strain and temperature compensation over a year period. Ciang et al. [7] provided a review of damage detection methods in 2008 and demonstrated that FBG sensors can be used for global blade monitoring. In 2012, Schubel et al. [8] provided a review of potential structural health monitoring applications using FBG sensors and also demonstrated the use of FBGs for improving composite cure process.

II. Methods

In 2017, a wake steering controller was tested at the DOE/Sandia SWiFT facility on an upstream and downstream pair of wind turbines, as shown in the middle and right of Figure 1. The experiment acquired synchronized structural and aerodynamic measurements for upstream, downstream, and throughout the wind turbine system. Critical measurements for this work were the FBG strain and temperature sensors within the rotor blades and a scanning LIDAR mounted within the nacelle pointing downwind. The FBG sensors, as shown in Figure 2, were located at the root of the rotor blade at the low-pressure (LP), trailing-edge (TE), high-pressure (HP) and leading-edge (LE) positions relative to the global blade coordinate system to measure strain for flap-wise and edge-wise bending. Temperature sensors were located at the root at the LP and HP positions to measure structural temperature and to compensate for thermal strain. In addition, data from the rotor instrumentation, the turbine pitch position, azimuth angle, tower bending, yaw angle, rotor speed, rotor torque and rotor power data channels were used for the analysis. The inflow velocity, direction, and yaw misalignment was calculated from the sensors on the meteorological tower located 2.5 diameters to the south of the dominantly upstream turbine, which has a rotor diameter of 27 meters.

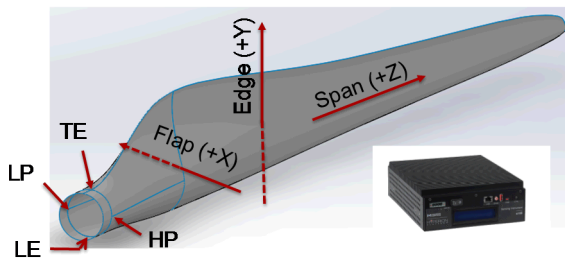


Figure 2. Strain and temperature sensor locations relative to blade coordinate system. Micron Optics Hyperion Interrogator (inset).



Figure 1. DOE Sandia SWiFT Facility.

FBG data was acquired with a Micron Optics Hyperion si155 Optical Sensing Interrogator that was made available through a partnership between SNL and Micron Optics supported by the DOE Small Business Voucher program. The si155 is a 4-channel offering of the x55 instrument technology with the ability to scan over a 160 nanometer wavelength range with 1 picometer absolute amplitude accuracy at 1 kHz sample rate [9]. The fanless and robust system is well suited for deployment within an operating wind turbine. Installed within one of the SWiFT turbine hub data acquisition enclosures, the Hyperion acquired data while rotating with the blades and transmitted the processed data back

to the nacelle where it was merged with the site-wide synchronized data.

Measurement of wind turbine blade operational strain, or total strain, includes an offset in strain typically resulting from the sensor installation process, a varying thermal strain due to the outdoor environmental temperature, a gravitational strain caused by the weight moment of the blade, and strains from wind loading in the flap and edge directions. Equation 2 shows a representation of total strain where CTE is the coefficient of thermal expansion and ΔT is the change in temperature. The quantity of interest for this work is the strain caused by wind loading, particularly as it relates to the yaw offset angle for wake steering. A method was developed to remove the mechanical offset, thermal, and gravitational strains from the total strain, thereby, providing an estimate of the strains exclusively caused by wind loading. Worth noting is that in a traditional foil strain gage both the offset and thermal strains can be corrected through a bridge, but FBG sensors are not deployed in bridges and so corrections must be done using an independent temperature measurement during post-processing. Previous work has also shown that thermal compensation using strain gage bridges may also be challenging as wind turbine blade materials are typically anisotropic [10].

$$\begin{aligned} \varepsilon_{Total} &= \varepsilon_{Thermal} + \varepsilon_{Mechanical\ Offset} + \varepsilon_{Gravitational} + \varepsilon_{Aerodynamic} \\ &\text{with } \varepsilon_{Thermal} = CTE * \Delta T \end{aligned} \quad (2)$$

Figure 3 illustrates the process developed for removing mechanical offset, thermal and gravitational strain and performing moment calibration in an operating wind turbine. The FBG system used in this work measures a reflected wavelength from FBGs within each sensor. The first step of the process is to convert the FBG wavelengths into measurements of total strain and absolute temperature. In the next step, data segments are identified with the turbine in favorable conditions to isolate thermal, mechanical offset and bending moment calibrations. For thermal strain, ideal conditions are a stationary rotor and low winds over a period of days. For mechanical offset and bending moment, ideal conditions are the turbine slowly rotating (less than 5 revolutions per minute to minimize centrifugal forces) in a feathered position in low winds. In the next step and utilizing the thermal strain segments, a least-squares first order polynomial is fit through each strain sensor and utilizing the most representative temperature sensor. For the leading and trailing edge strain sensors, the average of the low and high pressure temperature sensor was used. The slope of the polynomial fit is the Coefficient of Thermal Expansion (CTE) in units of microstrain per degree Celsius. The CTEs for this blade ranged from 10.3 to 11.7 microstrain per Celsius with a spread of 10-15% that illustrates the need for in-situ calibration instead of purely analytical estimation.

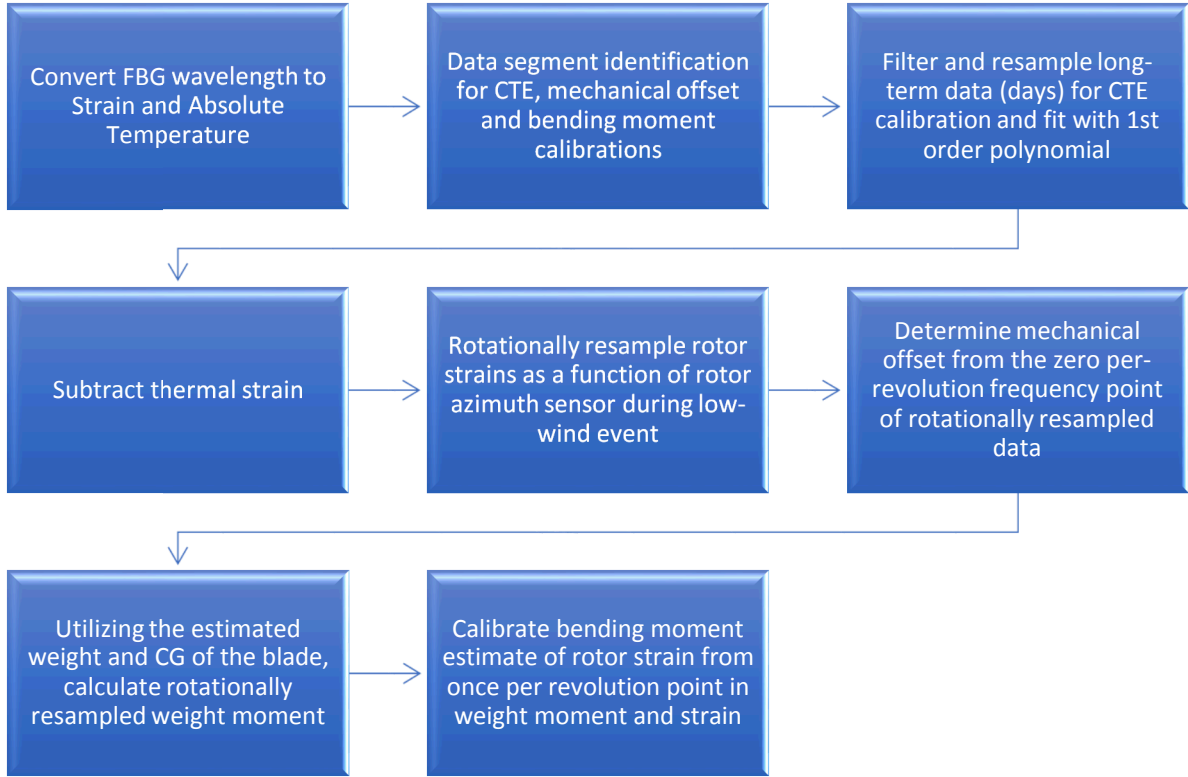


Figure 3. Strain data correction and calibration flow chart.

With the CTE estimated, the thermal strain can be estimated as a function of structural temperature and then the thermal strain can be subtracted from the total strain. Rotational-domain sampling was used for the next corrections. Rotational sampling is similar to common time-domain sampling where data is collected with a constant time-step and the inverse of the time-step is known as the sampling rate. In rotational sampling, data is acquired with a constant rotational-step and, in this case, would be the specific incremental angle of the rotation of the rotor. In this experiment, data were acquired in the time domain. To convert to the rotational domain, the time domain data were digitally resampled using the turbine azimuth encoder (sensor which measures the rotor rotation angle in 0 to 360 degrees). In the rotational-domain an estimate of the frequency domain using the Fourier transform has the form:

$$X(\omega_\theta) = \sum_{n=1}^N x(\theta) e^{(-\frac{i2\pi(k-1)(n-1)}{N})} \quad (2)$$

where ω_θ is the rotational frequency vector, $X(\omega_\theta)$ is the Fourier coefficients (frequency) in the rotational domain, N is the number of discrete data points, and $x(\theta)$ is the resampled rotational-domain data. Frequency content of the rotational-domain data provides many unique insights. Magnitude and phase of the Fourier coefficients both have meaning. Magnitude indicates the amplitude of a rotational-sinusoid at each frequency and the phase indicates where the magnitude has a maximum in the 0 to 360 degree rotation of the rotor. Zero-rotational-frequency (0P) point of the frequency domain indicates the average or quasi-static data value. The 1, 2, 3, etc.-per-revolution (1P, 2P, 3P, etc.) frequency points indicate sinusoids that occur one, two, three, etc. times per revolution with the phase indicating where in the revolution the positive magnitude occurs.

A comparison of the frequency content from time and rotational domain sampling is shown in Figure 4 for the torque and thrust directions on the turbine blade plotted with a similar frequency vector. The time-domain frequency data for torque less than 1P and approximately 1 Hz, illustrates the varying torque associated with varying speed of the wind turbine. The rotational domain frequency shows a distinct per-revolution peak for 0P, 1P, 2P, 3P, 4P, 5P and 6P. The rotational domain distinct peaks represent unique magnitude and phase information, whereas the time domain content can only be integrated for magnitude and does not contain any phase information.

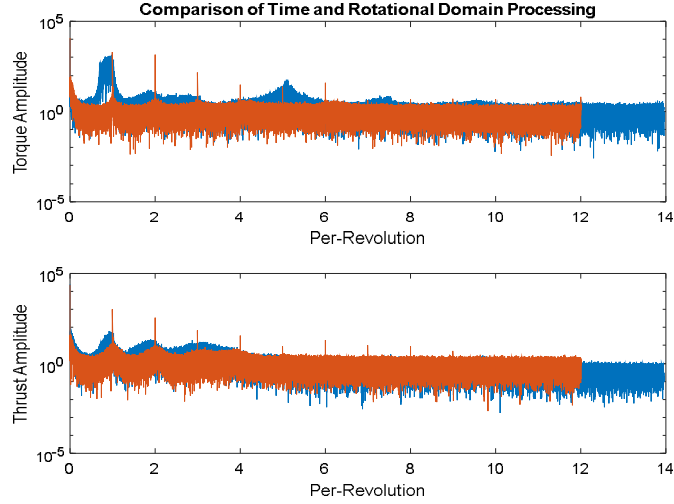


Figure 4. Comparison of time (blue) and rotational (red) domain processing of torque and thrust moment estimates.

Utilizing the frequency content of the rotational-domain the 0P and 1P of the appropriate data segments can be used to estimate the mechanical offset and gravitational strain. The mechanical offset strain estimate can be directly subtracted from the total strain. The gravitational strain can also be subtracted once a model for the gravitational strain as a function of azimuth and blade pitch angle is constructed. With thermal, gravity and offset strains removed, root strains can be used to estimate the aerodynamic source of the bending moment. To calibrate the bending moment the known weight moment comprised of the blade mass and center of gravity is used. The approximate relationship between bending moment and differential microstrain is 700 Newton meter (N·m) per microstrain. In later analysis, moment will be presented but it is worth noting that the 0P maximum magnitude is around 30-40 microstrain, 1P and 2P are 2-3 microstrain, and 3P is 0.5 microstrain. In terms of normal strain measurements these magnitudes are very low, particularly when compared with thermal strain swings of hundreds of microstrain.

Implementing this process, as shown in Figure 5, the total strain is converted into a bending moment. Figure 5b illustrates strain after the thermal strain and mechanical offset is removed. Bending moment is estimated in Figure 5c and with gravitational strain removed is shown in Figure 5d.

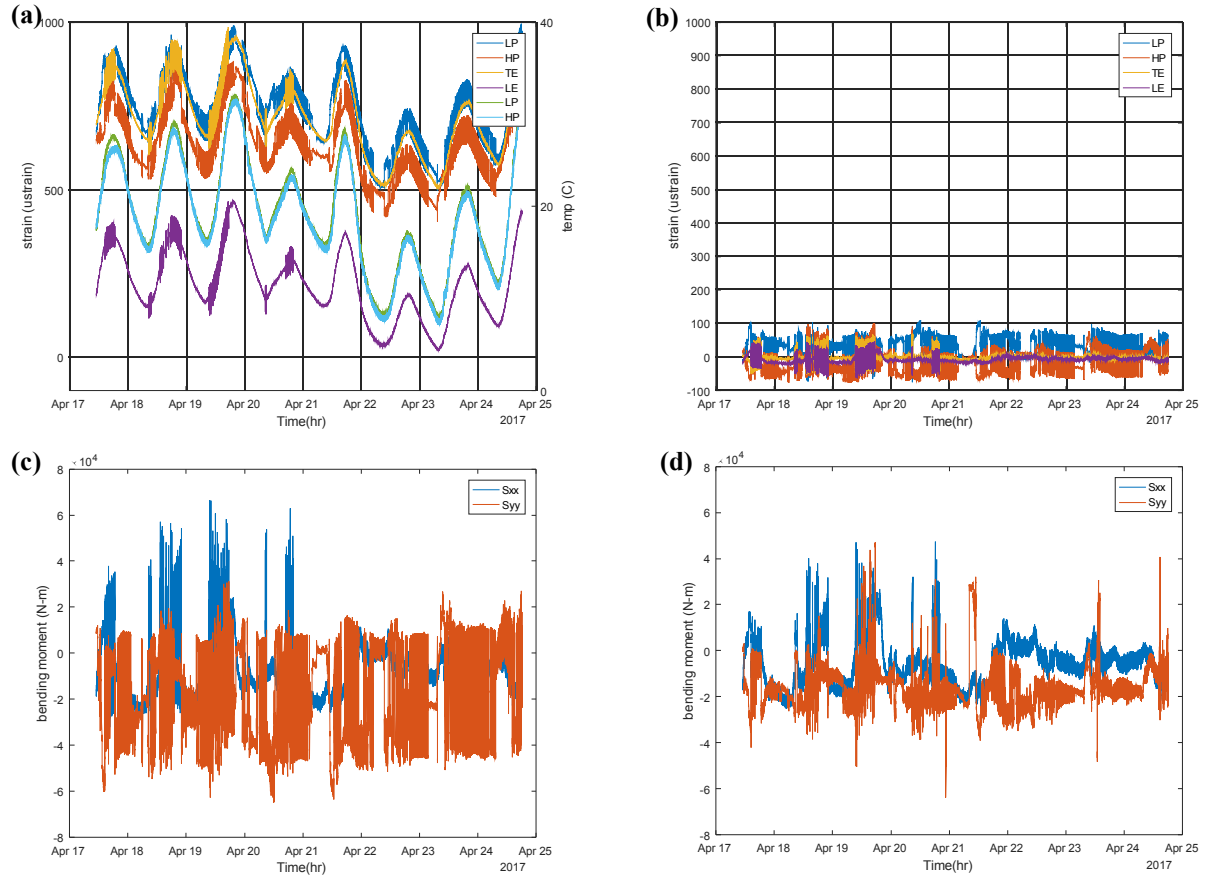


Figure 5. (a) Total strain, (b) thermal and offset corrected strain, (c) total bending moment estimation and (d) bending moment with gravity effect removed for the upwind SWiFT turbine.

III. Results

During 2017 a wake steering experiment was performed at the SWiFT Facility. For this analysis three unique data acquisition periods: July 12 0:00-4:00, July 12 4:30-8:30, and July 13 22:00-1:00 Central Standard Time were used. The yaw offset angle, power and wind speed are shown in Figure 6 for data period July 12 0:00-4:00. The yaw offset in this particular recording was stepped 0, 5, 10, 15, 20, 25, -10 and -5 degrees. The power production starts at approximately 50 kilowatt (kW), increases to 100 kW and then reduces to 20 kW. For the SWiFT turbines, the torque and speed is varied with wind speed when the generator torque is below 500 N·m. When torque is above 500 N·m the turbine control varies torque only. In this data period, the 32 meter (hub-height) wind speed increased from approximately 7, to 8, and then 6 meters per second. The 18 and 45 meter height wind speeds, corresponding to the bottom and top of the rotor, exhibited a vertical wind shear.

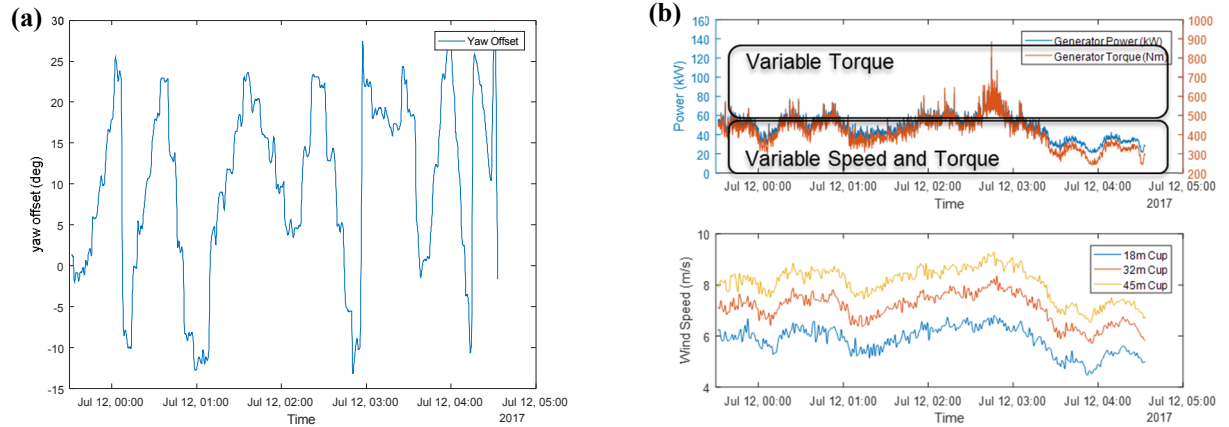


Figure 6. (a) Yaw offset angle, (b) power and wind speed while operating a wake steering controller on July 12 00:00 – 04:00 CST at the SWiFT Facility.

Applying the correction and calibration process previously discussed, estimates of the per-revolution magnitude and phase of the thrust and torque moment were estimated. For the rotational domain Fourier transform, 100 blade rotations (approximately 2 minutes) were used with an overlap of one rotation. These estimates were compared with the yaw offset (wake steering) angle to identify simple correlations, i.e. single variable relationships. The 0P estimate represents the quasi-static torque and thrust moment, shown in Figure 7. The yaw offset for the data recording is also shown in Figure 7, plotted against the second y-axis. A comparison of both moment and yaw offset does not appear to show a single variable correlation. A correlation is expected between yaw offset and thrust and torque moment, but would involve additional variables not accounted for in a two variable comparison. The phase angle of the 0P Fourier coefficient is not presented because it is always zero and does not provide insight.

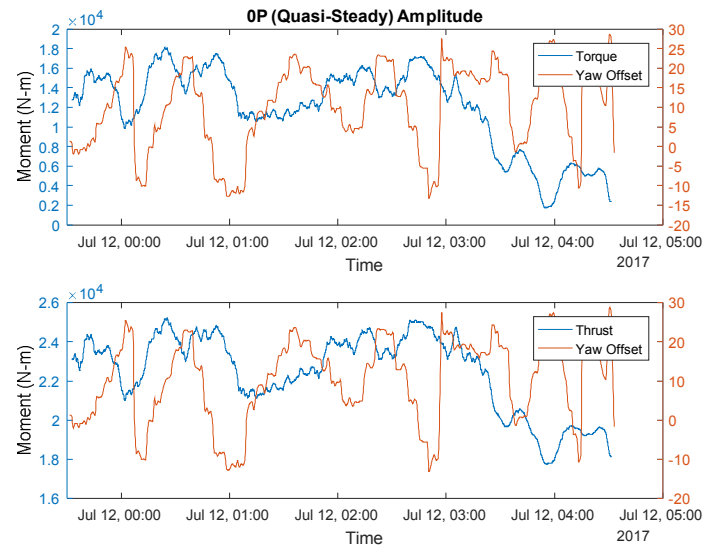


Figure 7. Quasi-steady amplitude of torque and thrust moment in relationship to yaw offset angle.

The 1P magnitude and phase of the thrust moment is shown in Figure 8. The magnitude of the moment indicates an inverse relationship with yaw offset. In this relationship when yaw offset increases in a positive direction the magnitude of the 1P thrust moment decreases and when the yaw offset increases in a negative direction the magnitude of the 1P thrust moment increases. A yaw offset range of -10 to 20 degrees appears to vary the magnitude from 800 N·m to 1400 N·m. The correlation appears to be stronger when the turbine is varying torque and speed (refer to Figure 6b).

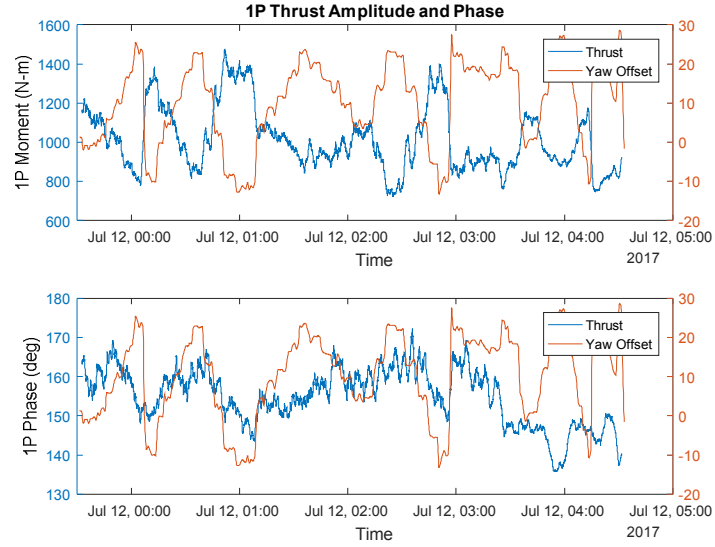


Figure 8. One-per-revolution thrust amplitude and phase in relationship to yaw offset angle.

The 2P magnitude and phase of the torque moment is shown in Figure 9. In this comparison, there does not appear to be a correlation between yaw offset and magnitude; however, there is a strong correlation between yaw offset and the phase of the 2P torque moment. A positive correlation is evident such that the phase angle increases with increasing yaw offset. In other words, increasing yaw offset angle of 20 degrees causes the two-per-revolution torque moment to occur 7 degrees forward in the blade rotation from vertical. Also, worth noting is that the correlation appears to be the most significant when the turbine is only varying torque.

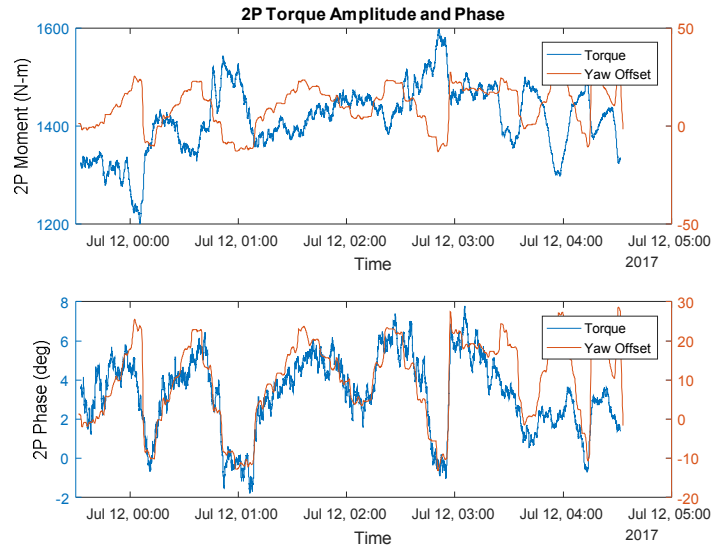


Figure 9. Two-per-revolution torque amplitude and phase in relationship to yaw offset angle.

The 3P magnitude and phase of the torque moment is shown in Figure 10. Similar to 2P there appears to be a positive correlation between yaw offset and 3P torque phase and a negative correlation between yaw offset and 3P torque magnitude. The range of the torque phase change is approximately 20 degrees to 70 degrees, which is a more significant change due to yaw offset. The correlation between torque phase and yaw offset appears to change when the turbine is varying speed and torque.

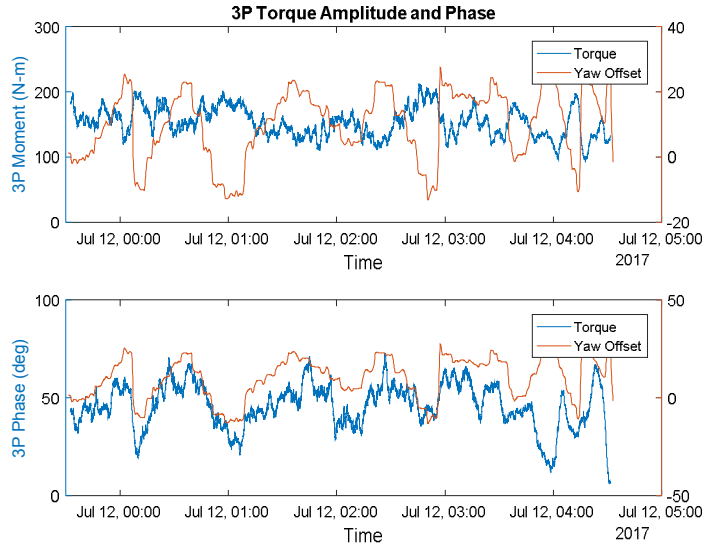


Figure 10. Three-per-revolution torque amplitude and phase in relationship to yaw offset angle.

To further investigate the previous relationships, the correlated variables were individually compared with yaw offset angle. Figure 11 shows the comparison of 1P thrust magnitude and yaw offset angle. A negative linear correlation is evident as previously stated and the segments where the turbine is operating with only variable torque appears to have less variability in the correlation.

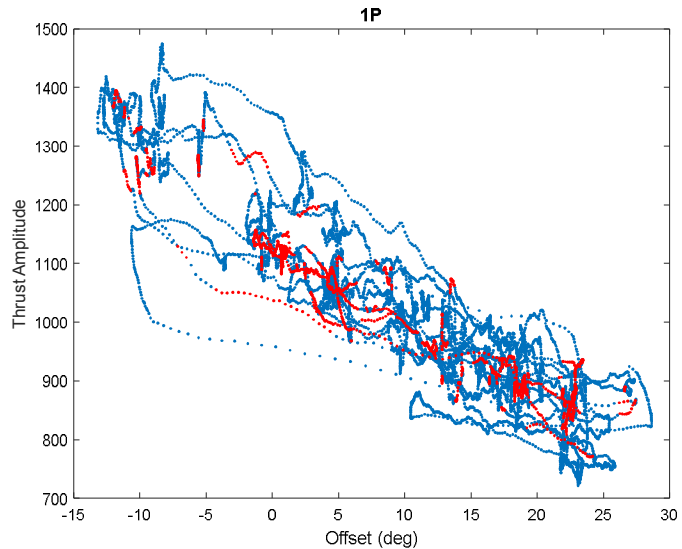


Figure 11. Correlation of one-per-revolution thrust amplitude and yaw offset angle where blue is variable speed and red is variable torque.

Figure 12 shows the correlation between 2P torque phase (a) and 3P torque phase (b) and yaw offset angle. 2P torque phase indicates a positive linear correlation with a small change in phase angle as previously noted. The region when the turbine is only varying torque appears to correlate with some of the outlier data, although additional outlier segments are evident. 3P torque phase also indicates a positive linear correlation.

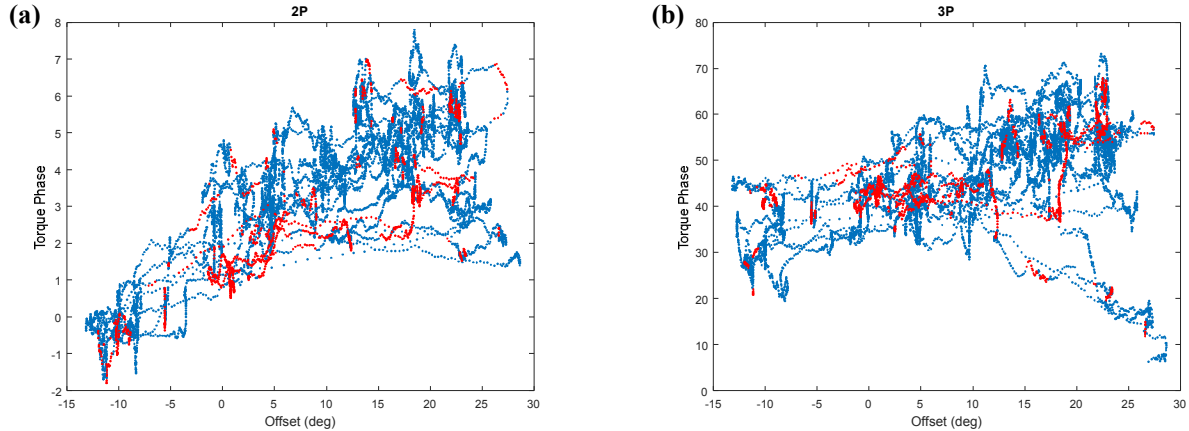


Figure 12. (a) Two-per-revolution and (b) three-per-revolution torque phase and yaw offset angle where blue is variable speed and torque and red is variable torque.

The same analysis was performed on the two other data sets from July 12 4:30-8:30 and July 13 22:00-1:00. The results of that analysis supported the finding presented from the first data set with similar phenomenon observed. Additionally, other per-revolution comparisons of yaw offset with thrust and torque magnitude and phase did not appear to have a single variable correlation.

IV. Conclusion

In this work, a data correction process with rotational-domain signal processing using a Fourier transform was shown to be an accurate and sensitive estimator of per-revolution thrust and torque moment magnitude and phase. FBG sensors may be capable of estimating quantities of interest at the single microstrain level when properly calibrated and corrected. Further, FBG when tied to the data process presented and the SWiFT data acquisition network have demonstrated the potential to acquire detailed quantities of interest in very short durations of hours instead of the common practice of acquiring months of data.

The intent of this work was to develop and demonstrate a data acquisition and analysis method, significant further work will be performed to use these methods to study the intricate physics that occur while attempting to steer wakes. Relationships to be developed should explain the correlations identified in this work and possibly additional multi-variable correlations not investigated within this work.

Acknowledgments

The work described in this paper was made possible by funding from the DOE Energy Efficiency and Renewable Energy's Wind Energy Atmosphere to Electrons (A2e) Program, the DOE Small Business Voucher Program and a partnership with Micron Optics. The data utilized for this work were made possible by the efforts of Jonathan Berg, Joshua Bryant, Miguel Hernandez, Christopher Kelley, David Mitchell and staff from NREL.

References

- [1] T. Herges, D. Maniaci and B. Naughton, "Scanning Lidar Spatial Calibration and Alignment Method for Wind Turbine Wake Characterization," in *35th Wind Energy Symposium, AIAA SciTech Forum*, Grapevine, 2017.
- [2] P. Fleming, M. Churchfield, A. Scholbrock, A. Clifton, S. Schreck, K. Johnson, A. Wright, P. Gebraad, J. Annoni, B. Naughton, J. Berg, T. Herges, J. White, T. Mikkelsen, M. Sjoholm and N. Angelou, "Detailed field test of yaw-based wake steering," *The Science of Making Torque from Wind (TORQUE 2016), Journal of Physics: Conference Series*, vol. 753, no. 2016, pp. 1-13, 2016.
- [3] J. Berg, J. Bryant, B. LeBlanc, D. Maniaci, B. Naughton, J. Paquette, B. Resor, J. White and D. Kroeker, "Scaled Wind Farm Technology Facility Overview," in *32nd ASME Wind Energy Symposium, AIAA SciTech Forum*, National Harbor, 2014.
- [4] L. Lading, M. McGugan, P. Sendrup, J. Rheinlander and J. Rusborg, "Fundamentals for Remote Structural Health Monitoring of Wind Turbine Blades - a Preproject," Riso National Laboratory, Roskilde, Denmark, 2002.

- [5] T. Verbruggen, "Wind Turbine Operation & Maintenance based on Condition Monitoring," ECN-C--03-047, 2003.
- [6] K. Schroeder, W. Ecke, J. Apitz, E. Lembke and G. Lenschow, "A fibre Bragg grating sensor system monitors operational load in a wind turbine rotor blade," *Measurement Science and Technology*, vol. 17, no. 2006, pp. 1167-1172, 2006.
- [7] C. C. Ciang, J.-R. Lee and H.-J. Bang, "Structural health monitoring for a wind turbine system: a review of damage detection methods," *Measurement Science and Technology*, vol. 19, no. 2008, p. 20, 2008.
- [8] P. Schubel, E. Crossley, J. Boateng and J. Hutchinson, "Review of structural health and cure monitoring techniques for large wind turbine blades," *Renewable Energy*, vol. 51, no. 2013, pp. 113-123, 2012.
- [9] T. Haber, "Micron Optics Announces Major Product Expansions to its HYPERION Platform," 25 June 2015. [Online]. Available: <http://www.prweb.com/releases/2015/06/prweb12811073.htm>.
- [10] W. D. Musial, M. D. Jenks and C. P. Butterfield, "A Simplified Method For Strain-Gage Temperature Compensation On Anisotropic Materials," SERI, Golden, CO, 1990.